Environ. Sci. Technol. **2004**, *38,* 3746−3751

Utilization of Solar Energy in the Photodegradation of Gasoline in Water and of Oil-Field-Produced Water

JOSÉ ERMÍRIO F. MORAES,[†] DOUGLAS N. SILVA,[†] FRANK H. QUINA,[‡] OSVALDO CHIAVONE-FILHO,*[,§] AND CLÁUDIO AUGUSTO O. NASCIMENTO[†]

Departamento de Engenharia Química, Escola Politécnica, Universidade de São Paulo, Cidade Universitária, São Paulo, 05508-900, SP, Brazil, Instituto de Química, Universidade de São Paulo, CP 26077, São Paulo, 05513-970, SP, Brazil, and Departamento de Engenharia Química, PPGEQ, Universidade Federal do Rio Grande do Norte, Campus Universitário, Lagoa Nova, Natal, 59072-970, RN, Brazil

The photo-Fenton process utilizes ferrous ions (Fe^{2+}), hydrogen peroxide (H_2O_2), and ultraviolet (UV) irradiation as a source of hydroxyl radicals for the oxidation of organic matter present in aqueous effluents. The cost associated with the use of artificial irradiation sources has hindered industrial application of this process. In this work, the applicability of solar radiation for the photodegradation of raw gasoline in water has been studied. The photo-Fenton process was also applied to a real effluent, i.e., oil-field-produced water, and the experimental results demonstrate the feasibility of employing solar irradiation to degrade this complex saturated-hydrocarbon-containing system.

Introduction

There are many sources of contamination of water resources, one of the most important being the emission of industrial effluents. These effluents may contain chemical components of high toxicity and frequently are not treatable by biological methods. Conventional physical−chemical methods may remove the pollutants from the aqueous phase, but do not destroy them, resulting in a problem of subsequent disposal of these contaminants (*1*−*3*).

New technologies have been developed with the goal of treating industrial effluents. Among these technologies, advanced oxidation processes (AOP) are of special prominence. These processes are characterized by the generation of the hydroxyl radical ($OH^{\bullet}$), which is a powerful, relatively unselective oxidizing agent (E^0 =2.8 V) that can oxidize practically all organic substances (*4*). The mode and site of the generation of the hydroxyl radical is what differentiates the various AOPs. In general, hydroxyl radicals or their equivalent are formed by UV irradiation of an oxidizing agent such as hydrogen materials like titanium dioxide (*5*).

The photo-Fenton process is one of the more widely studied AOPs. In the literature (*6*, *7*), detailed chemical mechanisms have been proposed. In the classical mechanism, hydroxyl radicals are generated by the cycle of oxidation and reduction reactions (outlined in eqs 1 and 2) that requires the presence of ferrous ions (Fe^{2+}), hydrogen peroxide (H_2O_2), and UV irradiation. In the first step, ferrous ions are oxidized by H_2O_2 (Fenton reaction), generating hydroxyl radicals (eq 1). In the second step, the ferric ions (Fe^{3+}) are reduced photochemically to the initial oxidation state (Fe^{2+}), producing an additional hydroxyl radical, which reacts again via eq 1 as long as H_2O_2 is available (*8*, *9*).

$$Fe^{2+} + H_2O_2 \rightarrow Fe^{3+} + OH^- + OH^{\bullet} \quad (1)$$

$$Fe^{3+} + H_2O \xrightarrow{h\nu} Fe^{2+} + H^+ + OH^{\bullet} \quad (2)$$

To the extent that it is a homogeneous AOP system, the photo-Fenton process presents no limitations of mass transfer, favoring the kinetics of degradation relative to heterogeneous systems such as TiO_2/UV (*10*). In some cases, the concentration of iron used in the photo-Fenton system may exceed the limit established by environmental legislation and may require removal of the ferric or ferrous ions at the end of the process.

An important barrier to industrial applications of AOP is the elevated cost of installing, operating, and maintaining artificial sources of UV radiation such as ionizers or lamps (*11*). Previous experiments on the degradation of raw gasoline in aqueous media demonstrated the feasibility of conducting the photo-Fenton process with medium-pressure mercury vapor lamps as the irradiation source. This suggested the possibility of using solar irradiation as the source of photons in this process. In this work, the application of solar energy for raw gasoline degradation via the photo-Fenton process has been studied. The experiments were carried out in a falling film type solar reactor, employing a complete two-level experimental design with three repetitions of the central point. Three concentration variables were analyzed, i.e., iron (Fe^{2+}) from 0.5 to 1.0 mM, total added hydrogen peroxide (H_2O_2) from 100 to 200 mmol/L of reaction, and sodium chloride (NaCl) from 200 to 2000 ppm.

Finally, the photo-Fenton process was applied to a real effluent with characteristics similar to the raw gasoline synthetic wastewater system. These experiments were carried out with waters produced in petroleum fields in Rio Grande do Norte State (Brazil). Solar radiation data were also recorded during all experiments to include the effect of this parameter on the kinetics of the degradation.

Experimental Methodology

Materials. Ferrous sulfate heptahydrate ($FeSO_4 \cdot 7H_2O$) and hydrogen peroxide (H_2O_2; 30%) were used as the source of hydroxyl radicals. Raw gasoline from a refinery was employed as the model pollutant and oil-field-produced water, collected from oil fields located in the State of Rio Grande do Norte (Brazil), was chosen as the real wastewater study case. The salinity of the gasoline system and the pH of the medium were adjusted with sodium chloride (NaCl) and concentrated sulfuric acid (H_2SO_4), respectively. In the experiments with gasoline, samples of the reaction mixture were withdrawn at different reaction times and a quenching solution containing potassium iodide (KI; 0.1 M), sodium sulfite (Na_2SO_3; 0.1 M), and sodium hydroxide (NaOH; 0.1 M) was added to stop the reaction. In the experiments with the oil-field-produced water, *n*-heptane (99.97%) was used to extract the organic

* Corresponding author phone: +55-84-215-3773, ext. 216; fax: +55-84-215-3770; e-mail: osvaldo@eq.ufrn.br.

[†] Departamento de Engenharia Química, Universidade de São Paulo.

[‡] Instituto de Química, Universidade de São Paulo.

[§] Universidade Federal do Rio Grande do Norte.

10.1021/es034701i CCC: $27.50
Published on Web 05/28/2004

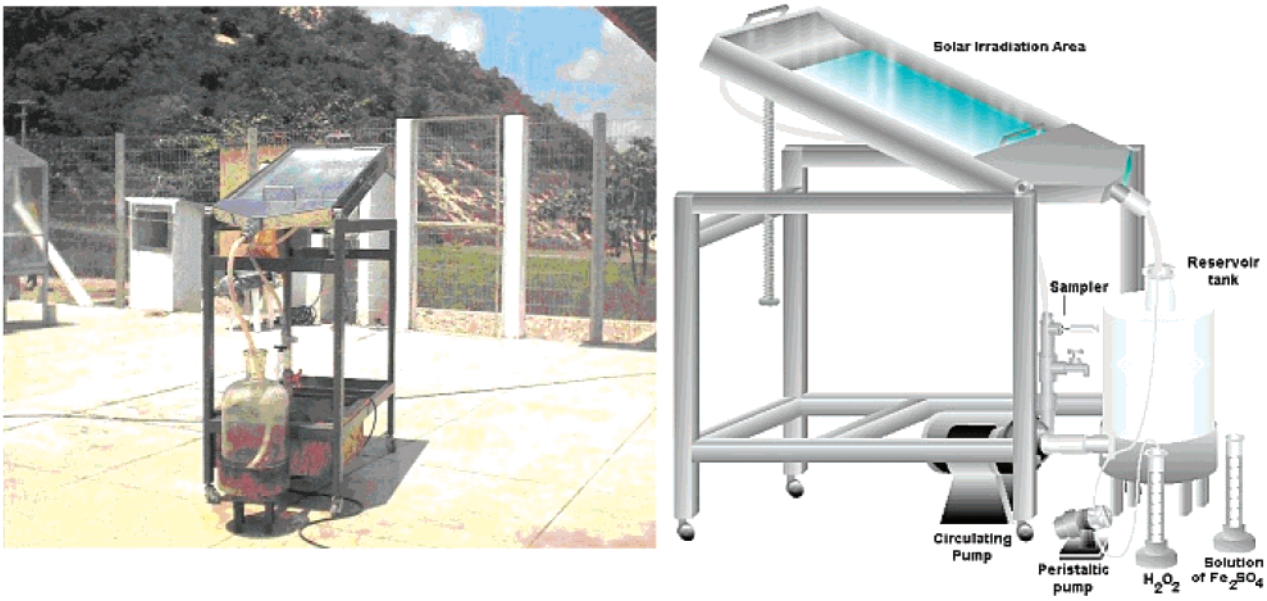

FIGURE 1. Photograph and scheme of the solar photochemical reactor (falling film type).

compounds present in the aqueous samples for posterior gas chromatographic analysis (GC).

Preparation of the Aqueous Gasoline Solutions. An 800-mL sample of raw gasoline and 8 L of distilled water were mixed vigorously during 4 h by mechanical stirring. The mixture was then left standing until complete separation of the liquid phases had occurred, usually overnight (ca. 12 h). The aqueous phase was then filtered twice through quantitative filter paper (2.0 μm), resulting in a reproducible initial concentration of organic carbon in the model wastewater (70−80 ppm C).

Apparatus. A falling film solar reactor of in-house construction (Figure 1) was employed. This photochemical reactor has a reservoir with a capacity of 10 L fitted with a mechanical stirrer. The reaction medium was recirculated through the reactor by means of a centrifugal pump. The reservoir, monitored by a digital thermometer, reached temperatures of up to 60 °C. Aqueous hydrogen peroxide was added to the system at the desired flow rate via a peristaltic pump.

The maximum collected solar irradiation area of the reactor is approximately 0.38 m^2 (45.4 cm wide × 83 cm high). The city of Natal (Rio Grande do Norte, Brazil) is located at a latitude of 5°42′ south of the equator. The collector surface was therefore oriented due north at an inclination of 15°42′. The additional 10° increment of the inclination above the latitude proved to be necessary to obtain an adequate draining of the falling film. To avoid exposure to irradiation, the reservoir was covered with black plastic film. The falling film reactor is fitted with a 4-mm-thick borosilicate glass cover, which serves to avoid evaporation, convection losses, and atmospheric contamination of the reaction medium during the experiments.

Experimental Procedure. In each experiment, 7.6 L of synthetic wastewater was prepared from raw gasoline. This solution was charged into the mixture tank and recirculated at a flow rate of ca. 17 L/min. The pH of the solution was adjusted to 3 by addition of concentrated sulfuric acid. The desired amount of sodium chloride, dissolved in 100 mL of distilled water, was then added and mixed into the system. The reaction was initiated by addition of 100 mL of an aqueous solution of $FeSO_4 \cdot 7H_2O$. Hydrogen peroxide solution (200 mL total volume) was added continuously via a peristaltic pump during the first 2 h of reaction. Table 1 lists the absolute and coded values assigned to the concentration variables included in the experimental design. Solution bulk temperature and solar irradiation intensity were recorded throughout the course of the reaction. The experiments were typically initiated at about 11:00 a.m. with a total period of reaction (solar exposure) of 4.5 h. Samples (5 mL) were withdrawn at fixed times and the quenching solution (2 mL) was added. The samples were filtered (0.22-μm Durapore Millipore membrane filter) to remove precipitated iron hydroxides before analysis of total organic carbon (TOC 5000-A, Shimadzu).

TABLE 1. Experimental Design Parameters for the Photodegradation of Raw Gasoline

	absolute level		
coded level	H_2O_2 (mmol/L reaction)[a]	Fe^{2+} (mM)	NaCl (mM)
−1	100	0.50	200
0	150	0.75	1100
+1	200	1.00	2000

[a] Total number of millimoles of H_2O_2 added to the reservoir per liter of reaction mixture.

Experimental Procedure for the Oil-Field-Produced Water. For the real effluent, the procedure consisted of charging the reservoir with 7.7 L of raw oil-field-produced water acidified to pH 3 with concentrated H_2SO_4. The photo-Fenton reaction was initiated by addition of 100 mL of an aqueous solution of $FeSO_4 \cdot 7H_2O$, followed by gradual addition of H_2O_2 over the first 2 h of reaction (200 mL total volume). Experiments were performed under the conditions indicated in Table 2.

Samples (100 mL) were collected during the 6-h period of solar exposure. Each sample was added to a separation funnel and 2 mL of pure *n*-heptane was added. The liquids in the funnel were mixed vigorously for one minute, allowed to stand for 60 min (*12*), and the organic phase was carefully removed using a Pasteur pipet for GC analysis on a gas chromatograph (GC-17A, Shimadzu) fitted with an autosampler (AOC-20i, Shimadzu) and a flame ionization detector (FID). A capillary column (Petrocol-DH, 100 m × 0.25 mm i.d., Df = 0.5 μm) was employed with a carrier gas (N_2) flow rate of 3 mL/min. The temperature programming of the column was the following: the initial temperature of 35 °C was maintained for 15 min, then raised to 60 °C at a rate of

TABLE 2. Experimental Conditions Used in the Photodegradation of Oil-Field-Produced Water

experimental condition	H_2O_2 (mmol/L reaction)[a]	Fe^{2+} (mM)
1[b]		
2	100	1
3	200	1
4	300	1

[a] Total number of millimoles of H_2O_2 added to the reservoir per liter of reaction mixture. [b] Photolysis was performed without ferrous ions or hydrogen peroxide.

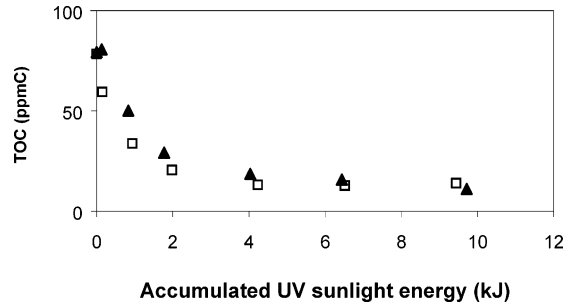

FIGURE 2. Influence of $[Fe^{2+}]$ on the photodegradation of raw gasoline in aqueous medium; $[H_2O_2] = 100$ mmol/L reaction and [NaCl] = 200 ppm: □ $[Fe^{2+}] = 1.0$ mM; ▲ $[Fe^{2+}] = 0.5$ mM; accumulated solar energy, in kJ, was calculated by integrating data at 305, 320, 340, and 380 nm over each time interval and multiplying by the exposed area of the solar reactor (0.38 m^2).

1 °C/min, maintained at this temperature for 20 min, then increased to 200 °C at a rate of 2 °C/min, and finally increased to 250 °C at a rate of 10 °C/min. The temperatures of the injector and detector (FID) were set to 300 °C. Total volatile organic content, in ppm, was estimated from the total area of the chromatogram assuming that the FID response is directly proportional to the carbon number of the organic constituents.

Results and Discussion

Experimental Design. All of the experiments were carried out under similar conditions of solar irradiation, i.e., on relatively cloudless days to minimize differences in the kinetics of degradation due to widely different experimental conditions of photon flux. The temperature of the system was not controlled and varied between 25 and 60 °C according to the extent of solar exposure. This allowed evaluation of the system under real conditions of operation for wastewater treatment, where temperature control would increase cost unnecessarily. In a previous study of the degradation of phenol via the photo-Fenton process (*13*), it was shown that the temperature did not affect the average rate of degradation significantly in the range of 30−50 °C.

Influence of the Fe^{2+} Concentration. The effect of Fe^{2+} concentration on the degradation of raw gasoline using solar radiation was quite similar to that observed in experiments realized with an artificial UV light source. For fixed concentrations of H_2O_2 and NaCl, the experiments performed with the maximum level of Fe^{2+} presented the highest initial degradation rates, see Figure 2.

Influence of the H_2O_2 Concentration. The effect of hydrogen peroxide concentration was also similar to that observed in experiments with a UV lamp. Increasing the H_2O_2 concentration did not result in a directly proportional increase in the average degradation rate, but the highest levels of conversion were observed at the maximum value of this variable, as shown in Figure 3.

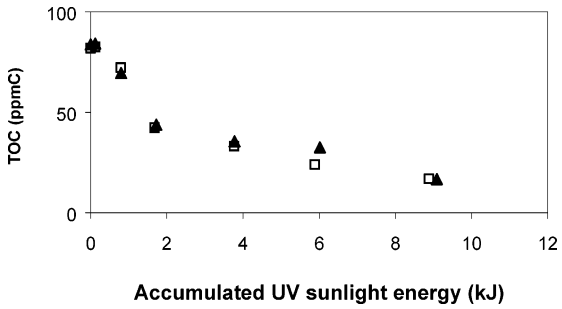

FIGURE 3. Influence of $[H_2O_2]$ on the photodegradation of the raw gasoline in aqueous medium; $[Fe^{2+}] = 0.5$ mM and [NaCl] = 2000 ppm: □ $[H_2O_2] = 200$ mmol/L reaction; ▲ $[H_2O_2] = 100$ mmol/L reaction; accumulated solar energy, in kJ, was calculated by integrating data at 305, 320, 340, and 380 nm over each time interval and multiplying by the exposed area of the solar reactor (0.38 m^2).

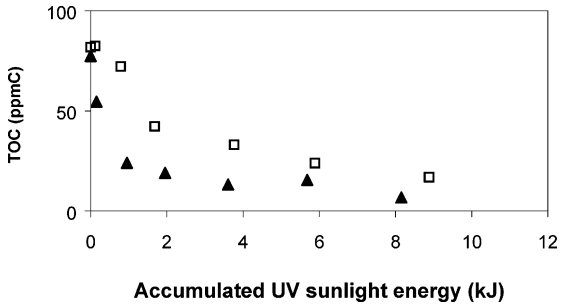

FIGURE 4. Influence of [NaCl] on the photodegradation of raw gasoline in aqueous medium; $[Fe^{2+}] = 1$ mM and $[H_2O_2] = 200$ mmol/L reaction: □ [NaCl] = 2000 ppm; ▲ [NaCl] = 200 ppm; accumulated solar energy, in kJ, was calculated by integrating data at 305, 320, 340, and 380 nm over each time interval and multiplying by the exposed area of the solar reactor (0.38 m^2).

Influence of the NaCl Concentration. The inhibitory effect of chloride anions (Cl^-), observed in experiments using an UV lamp, has been suggested to involve the formation of Fe^{3+} and Cl^- complex species (*6*, *14*, *15*). This complex formation, indicated in eqs 3 and 4, affects the photochemical reduction of Fe^{3+} and/or the net yield of hydroxyl radicals. On the other hand, the higher quantum yield (*15*) for photolysis of the $FeCl^{2+}$ complex ($\Phi_{347nm} = 0.5$), shown in eq 5, relative to $Fe(OH)^{2+}$ ($\Phi_{347nm} = 0.21$), eq 2, might, under the appropriate circumstances, reduce the effect of Cl^- on the photo-Fenton process, because of the increased efficiency of photocatalytic reduction of Fe^{3+} to Fe^{2+}.

$$Fe^{3+} + Cl^- \rightarrow FeCl^{2+} \quad (3)$$

$$Fe^{3+} + 2Cl^- \rightarrow FeCl_2^{+} \quad (4)$$

$$FeCl^{2+} \xrightarrow{h\nu} Fe^{2+} + Cl^{\bullet} \quad (5)$$

However, at the same time, electron transfer between chloride anions and hydroxyl radicals followed by proton transfer leads to the formation of chlorine radicals ($Cl^{\bullet}$) and $Cl_2^{\bullet-}$, according to eqs 6 and 7, which are less oxidative than hydroxyl radicals ($^{\bullet}OH$), an effect referred to as anion scavenging of hydroxyl radicals (*6*, *16*).

$$OH^{\bullet} + Cl^- \xrightarrow{H^+} Cl^{\bullet} + H_2O \quad (6)$$

$$Cl^{\bullet} + Cl^- \xrightarrow{H^+} Cl_2^{\bullet-} \quad (7)$$

Indeed, the effect of NaCl was more pronounced than that of any of the other variables examined. Figure 4 shows

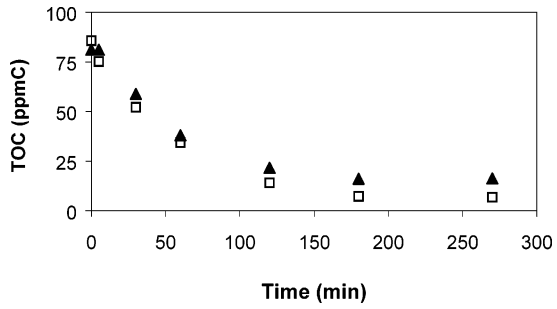

FIGURE 5. Qualitative comparison of solar and medium-pressure Hg lamp irradiation in raw gasoline degradation; $[Fe^{2+}] = 0.5$ mM, $[H_2O_2] = 200$ mmol/L reaction, and [NaCl] = 200 ppm: ▲ photolysis of 7.6 L of solution in the solar reactor (total accumulated solar energy of 9.2 kJ); □ photolysis of 2.2 L of solution with a 4-W Hg lamp in a conventional Pyrex immersion well and reactor (*16*), total lamp output, as determined by actinometry with 0.15 M potassium ferrioxalate (*17*), of 7×10^{-5} Ein/s.

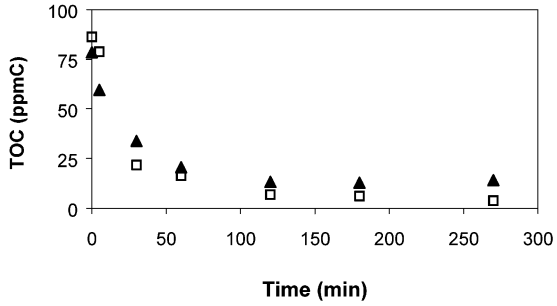

FIGURE 6. Qualitative comparison of solar and medium-pressure Hg lamp irradiation in raw gasoline degradation; $[Fe^{2+}] = 1$ mM, $[H_2O_2] = 100$ mmol/L reaction, and [NaCl] = 200 ppm: ▲ photolysis of 7.6 L of solution in the solar reactor (total accumulated solar energy of 9.2 kJ); □ photolysis of 2.2 L of solution with a 450-W Hg lamp in a conventional Pyrex immersion well and reactor (*16*), total lamp output, as determined by actinometry with 0.15 M potassium ferrioxalate (*17*), of 7×10^{-5}Ein/s.

the difference in the temporal variation of the TOC at two extremes of salinity under otherwise identical conditions.

Influence of the Solar Irradiation. Figures 5 and 6 show a comparison between experiments performed using solar and Hg lamp light reactors. Although the artificial source of UV light gave, in general, slightly better photodegradation than solar irradiation, as deduced from the TOC kinetic profiles, similar dependences were observed with respect to the concentrations of Fe^{2+}, H_2O_2, and NaCl. Solar irradiation intensities were monitored in all experiments. Table 3 summarizes the accumulated incident solar energy data for the collector surface of the reactor during the sampling period. Table 4 presents the experimental data for the total organic carbon as a function of reaction time for all gasoline photodegradation experiments in aqueous media.

Photo-Fenton Treatment Applied to Oil-Field-Produced Water. To test the applicability of the photo-Fenton process in a real case using solar radiation as the source of UV light, photodegradation experiments were performed with oil-field-produced wastewater from the Rio Grande do Norte State (Brazil). In all experiments, a visual change in the color of the oil-field produced water could be observed qualitatively during the photochemical treatment. Thus, the initially slightly cloudy, yellow mixture became transparent as the reaction proceeded. These transformations could be seen most clearly in the prepared samples, extracted with *n*-heptane, as shown in Figure 7.

In the absence of the Fenton reagents, irradiation resulted in an *increase* in the concentration of hydrocarbons in the aqueous phase, which accompanied the gradual increase in the temperature of the aqueous phase caused by absorption of the solar irradiation, as shown in Figure 8. This phenomenon is readily explained by the increase in the solubility of the hydrocarbons in water with increasing temperature.

The photo-Fenton experiments are indicative of the competition between two effects during the process. On one hand, the temperature increase provoked by the solar irradiation (thermal effect) favors the solubilization of organic compounds in suspension, increasing the concentration of dissolved hydrocarbons in the samples. At the same time, photodegradation reduces the organic content. Figure 9 demonstrates this interesting phenomenon in a case where H_2O_2 addition was interrupted between 30 and 60 min of reaction, resulting in a considerable increase in the dissolved organics of the solution in this period. Subsequently, the rest of the hydrogen peroxide solution was added in two equal parts, with a consequent rapid fall in the organic content.

This competition of thermal and photodegradation effects results in a complex behavior of the organic content as the reaction proceeds. At the beginning of the reaction, the rate of reaction was the highest, probably due to the rapid decomposition of the aromatic constituents, and photodegradation predominates over the thermal effect. With the increase in temperature, more hydrocarbons solubilize in the aqueous phase, increasing the content of organic compounds in this phase after all of the added H_2O_2 has been consumed. This behavior is illustrated in Figure 10. Table 5 lists the numerical values of the organic content as a function of the reaction time for all of the experiments performed with oil-field-produced water from Rio Grande do Norte State (Brazil).

Final Comments. The photodegradation experiments with synthetic wastewater prepared with raw gasoline confirm

TABLE 3. Accumulated Solar (UV) Radiation Data during the Gasoline Photodegradation Experiments

$[Fe^{2+}]$ (mM)	$[H_2O_2]$ (mmol/L reaction)[a]	[NaCl] (ppm)	accumulated UV energy (kJ) (305, 320, 340 and 380 nm)						
			0 min[b]	5 min[b]	30 min[b]	60 min[b]	120 min[b]	180 min[b]	270 min[b]
1	200	200	0	0.16	0.95	1.95	3.61	5.68	8.15
0.75	150	1100	0	0.02	0.31	1.02	2.67	4.77	7.67
1	100	2000	0	0.12	0.80	1.72	3.78	6.02	9.09
0.75	150	1100	0	0.12	0.83	1.79	3.96	6.26	9.48
0.5	200	200	0	0.16	1.01	2.03	4.28	6.46	9.16
1	100	200	0	0.15	0.93	1.97	4.23	6.51	9.44
1	200	2000	0	0.12	0.79	1.68	3.76	5.88	8.88
0.5	100	2000	0	0.14	0.84	1.80	3.86	5.93	9.03
0.5	200	2000	0	0.05	0.39	0.86	1.76	3.33	6.38
0.5	100	200	0	0.13	0.83	1.77	4.04	6.44	9.72
0.75	150	1100	0	0.16	0.80	1.80	4.38	6.81	10.16

[a] Total number of millimoles of H_2O_2 added to the reservoir per liter of reaction mixture. [b] Reaction time in minutes.

TABLE 4. Experimental TOC Data for Gasoline Photodegradation Employing Solar Radiation

$[Fe^{2+}]$ (mM)	$[H_2O_2]$ (mmol/L reaction)[a]	[NaCl] (ppm)	TOC (ppm C)						
			0 min[b]	5 min[b]	30 min[b]	60 min[b]	120 min[b]	180 min[b]	270 min[b]
1	200	200	77.43	54.68	24.19	19.11	13.31	15.64	6.86
0.75	150	1100	72.43	49.14	32.54	24.40	21.14	19.64	13.15
1	100	2000	83.75	84.14	69.50	43.83	35.57	32.59	16.78
0.75	150	1100	78.13	79.73	70.01	52.16	28.48	24.37	25.38
0.5	200	200	81.12	81.14	58.87	38.04	21.66	16.04	16.25
1	100	200	78.50	59.56	33.84	20.58	13.19	12.81	14.04
1	200	2000	81.87	82.57	72.17	42.36	33.19	24.08	16.98
0.5	100	2000	78.41	81.45	50.29	40.89	29.62	24.42	26.25
0.5	200	2000	79.32	81.09	57.88	35.50	19.92	16.42	15.36
0.5	100	200	79.40	80.79	50.19	29.22	18.65	15.86	11.13
0.75	150	1100	78.27	79.91	43.51	33.89	18.35	16.93	18.90

[a] Total number of millimoles of H_2O_2 added to the reservoir per liter of reaction mixture. [b] Reaction time in minutes.

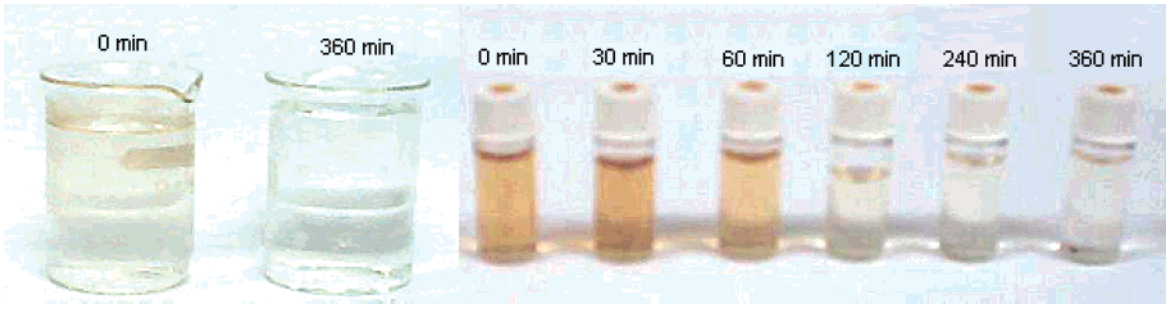

FIGURE 7. Visual appearance of the samples along the photochemical treatment of the oil-fie-produced water: (a) oil-field-produced water before and after the photo-Fenton process, and (b) samples extracted with *n*-heptane before GC analysis.

TABLE 5. Experimental Results Analyzed via Gas Chromatography for the Photodegradation of One Sample of Oil-Field-Produced Water

$[Fe^{2+}]$ (mM)	$[H_2O_2]$ (mmol/L reaction)[a]	organic content (ppm)						
		0 min[b]	5 min[b]	30 min[b]	60 min[b]	120 min[b]	240 min[b]	360 min[b]
		3.13		30.88				98.80
1	100	31.97	14.45	27.38	81.99	18.20	5.87	17.76
1	200	51.98		44.71	14.63	12.23	46.16	45.98
1	300	46.09	12.94	10.60	1.90		26.39	

[a] Total number of millimoles of H_2O_2 added to the reservoir per liter of reaction mixture. [b] Reaction time in minutes.

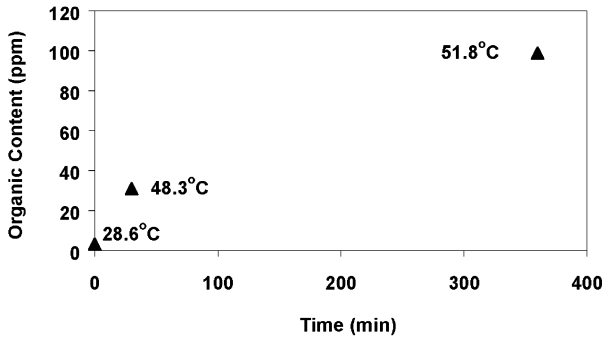

FIGURE 8. Photolysis of oil-field-produced water (without Fe^{2+} and H_2O_2) with solar radiation; the thermal effect of hydrocarbon solubilization is observed.

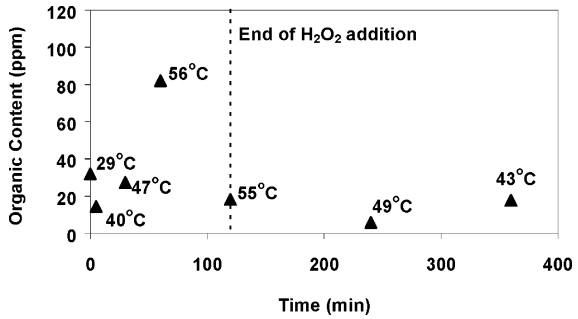

FIGURE 9. Photodegradation of the oil-field-produced water using solar radiation; $[Fe^{2+}] = 1$ mM and $[H_2O_2] = 200$ mmol/L reaction.

the strong inhibitory effect of chloride ions (Cl^-), which impeded complete mineralization. The inhibitory effect of chloride ions is quite important because real wastewaters often contain significant amounts of salts such as chlorides and carbonates. For instance, the oil-field-produced water studied here contains about 2000 ppm of chlorides.

In terms of yield, the raw gasoline photodegradation experiments showed that, on average, 60% of the initial organic content was mineralized in the first 3 h. After 4.5 h of solar exposition, the mineralization ranged between 66 and 91%. This information is relevant because such high yields of degradation would be compatible with application of the photo-Fenton system as a pretreatment for a subsequent biological degradation process. The results obtained for the oil-field-produced water also indicated the technical feasibility of the photo-Fenton system using solar radiation despite the solubility limitations.

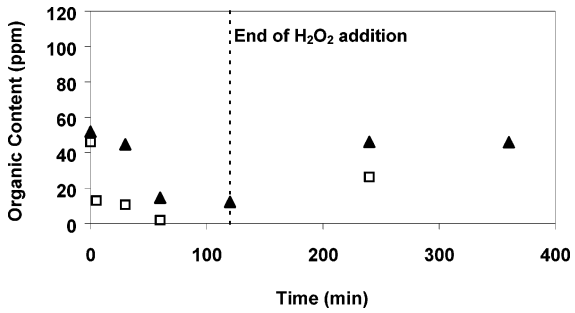

FIGURE 10. Photodegradation of two different oil-field-produced water samples (□ and ▲) irradiated in the solar reactor on different days: $[Fe^{2+}]$ = 1mM and $[H_2O_2]$ = 300 mmol/L reaction.

Acknowledgments

Financial support from CNPq (Conselho Nacional de Desenvolvimento Científico e Tecnológico), FAPESP (Fundação de Amparo à Pesquisa do Estado de São Paulo), ANP (Agência Nacional do Petróleo), and CAPES (Coordenação de Aperfeiçoamento de Pessoal de Nível Superior) is gratefully acknowledged. We also thank INPE (Instituto Nacional de Pesquisas Espaciais) for providing solar radiation data, GASOL/UFRN (Laboratório de Combustíveis da Universidade Federal do Rio Grande do Norte) for technical support in the gas chromatographic analyses, and Amilcar Machulek Jr. for performing the ferrioxalate actinometry.

Literature Cited

(1) De Villiers, M. *Water − Fate of our Most Precious Resource*; Houghton Mifflin: Boston, MA, 2001.
(2) Crittenden, J. C.; Suri, R. P. S.; Perram, D. L.; Hand, D. W. *Wat. Res.* **1997**, *31*, 411−418.
(3) Kim, S. M.; Geissen, S. U.; Vogelpohl, A. *Wat. Sci. Technol.* **1997**, *35*, 239−248.
(4) Malato, S.; Blanco, J.; Cáceres, J.; Fernández-Alba, A. R.; Agüera, A.; Rodríguez, A. *Catal. Today* **2002**, *76*, 209−220.
(5) Chen, H. Y. Etude Comparée de l'Adsorption et de la Dégradation Photocatalytique de Pollutants des Eaux, Ph.D. Thesis, l'Instituto National Polytechnique de Lorraine, France, 1994.
(6) Pignatello, J. J. *Environ. Sci. Technol.* **1992**, *26*, 944−951.
(7) Bossmann, S. H.; Oliveros, E.; Göb, S.; Siegwart, S.; Dahlen, E. P.; Payawan, L., Jr.; Straub, M.; Wöner, M.; Braun, A. M. *Phys. Chem.* **1998**, *102*, 5542−5550.
(8) Krutzler, T.; Fallmann, H.; Maletzky, P.; Bauer, R.; Malato, S.; Blanco, J. *Catal. Today* **1999**, *54*, 321−327.
(9) Kim, S.; Vogelpohl, A. *Chem. Eng. Technol.* **1998**, *21*, 187−191.
(10) Krutzler, T.; Bauer, R. *Chemosphere* **1999**, *38*, 2517−2532.
(11) Martyanov, I. N.; Savinov, E. N. *Catal. Today.* **1997**, *39*, 197−205.
(12) Peake, E.; Hodgson, G. W. *J. Am. Oil Chem. Soc.* **1966**, *43*, 215−222.
(13) Moraes, J. E. F.; Will, I. B. S.; Yu, J. N. W.; Teixeira, A. C. S. C.; Guardani, R. In *Proc. 3rd European Congress on Chemical Engineering, Nuremberg, 26−28 June 2001*; DECHEMA: Frankfurt A. M., 2001.
(14) Aplin, R.; Waite, T. D. *Wat. Sci. Technol.* **2000**, *42*, 345−354.
(15) Kiwi, J.; Lopez, A.; Nadtochenko, V. *Environ. Sci. Technol.* **2000**, *34*, 2162−2168.
(16) Moraes, J. E. F.; Quina, F. H.; Nascimento, C. A. O.; Silva, D. N.; Chiavone-Filho, O. Treatment of Saline Wastewater Contaminated with Hydrocarbons by the Photo-Fenton Process. *Environ. Sci. Technol.* **2004**, *38* (4), 1183−1187.
(17) Murov, S. L. *Handbook of Photochemistry*; Marcel Dekker: New York, 1973; p 119.

Received for review July 2, 2003. Revised manuscript received December 9, 2003. Accepted April 28, 2004.

ES034701I